

LA-UR-19-30139

Approved for public release; distribution is unlimited.

Title: Progress Toward an Indirect Neutron Capture Capability at LANSCE:
October 2018 – September 2019

Author(s): Koehler, Paul E.
Ullmann, John Leonard
Couture, Aaron Joseph
DiGiovine, Brad Joseph

Intended for: Report

Issued: 2019-10-07

Disclaimer:

Los Alamos National Laboratory, an affirmative action/equal opportunity employer, is operated by Triad National Security, LLC for the National Nuclear Security Administration of U.S. Department of Energy under contract 89233218CNA000001. By approving this article, the publisher recognizes that the U.S. Government retains nonexclusive, royalty-free license to publish or reproduce the published form of this contribution, or to allow others to do so, for U.S. Government purposes. Los Alamos National Laboratory requests that the publisher identify this article as work performed under the auspices of the U.S. Department of Energy. Los Alamos National Laboratory strongly supports academic freedom and a researcher's right to publish; as an institution, however, the Laboratory does not endorse the viewpoint of a publication or guarantee its technical correctness.

Progress Toward an Indirect Neutron Capture Capability at LANSCE: October 2018 – September 2019

P. E. Koehler, J. L. Ullmann, B. J. DiGiovine, and A. Couture

P-27, Los Alamos National Laboratory

Abstract: We describe progress developing the Device for Indirect Capture Experiments on Radionuclides (DICER) on flight path 13 at the Lujan Center at the Los Alamos Neutron Science Center (LANSCE). This capability is being developed to tightly constrain neutron-capture cross section on short-lived radioactive nuclides of high importance to weapons-program sponsors via neutron total cross section measurements on the same nuclides. In this report, we describe progress in this endeavor during October 2018 through September 2019.

I. Executive summary

During this period, the following progress was made. 1) A full LDRD DR proposal was submitted and selected for funding starting October 2019. 2) New data acquisition and replay computer systems were designed, purchased and installed. 3) Several more improvements were made to the apparatus. 4) A novel dual-hole sample collimation system was designed and simulated with MCNP and a precision five-axis positioning system is being developed to accurately align this device. 5) The expected uncertainties in the $^{88}\text{Y}(n,\gamma)$ cross section before (factor of 5 – 30) and after (5 – 14%) a DICER measurement were estimated. 6) DICER measurements on a thin cadmium sample were used to assess the feasibility of determining the position and width of the resonance responsible for the exceptionally large $^{88}\text{Zr}(n,\gamma)$ thermal cross section. Results indicate that measurements with a 1.1 μg , 1-mm diameter ^{88}Zr sample should require about one day of beam time. 7) A talk about DICER and related topics was presented at the 10th Tri-Lab Nuclear Data Workshop and a DICER paper was accepted for publication in the proceedings of the 6th Workshop on Compound Nuclear Reactions. Each of these topics is addressed in separate sections below.

II. New DICER LDRD DR proposal submitted and funded

Our LDRD DR proposal entitled “Predictive Understanding of Device Performance through Innovative Measurement, Modeling, and Simulation on Radiochemical Dosimeters” [1] was chosen for funding starting October 1, 2019. The main goal is to develop the DICER technique to the point where we have demonstrated feasibility through successful measurements on ^{88}Zr and ^{88}Y .

III. Upgraded data acquisition and replay computers

We designed, purchased and installed new data acquisition and replay computer system to facilitate more efficient experiment and data reduction operations.

IV. DICER apparatus improvements

The DICER apparatus was improved in three major ways.

First, the last remaining sections of neutron guide outside the Lujan-Center bulk shield (in the shutter and in the wall between experimental rooms 1 and 2) were removed and replaced with new collimation

and a filter box (see below). This improved the overall collimation of the beam and hence should improve the signal-to-noise ratio.

Second, a filter box was installed just downstream of the shutter. This apparatus will allow us to remotely insert and remove “filters” of CH₂, Bi, Pb, and Cd in the beam. These filters will be used to eliminate wrap-around neutrons and to measure backgrounds. A drawing of the filter box is shown in Fig. 1.

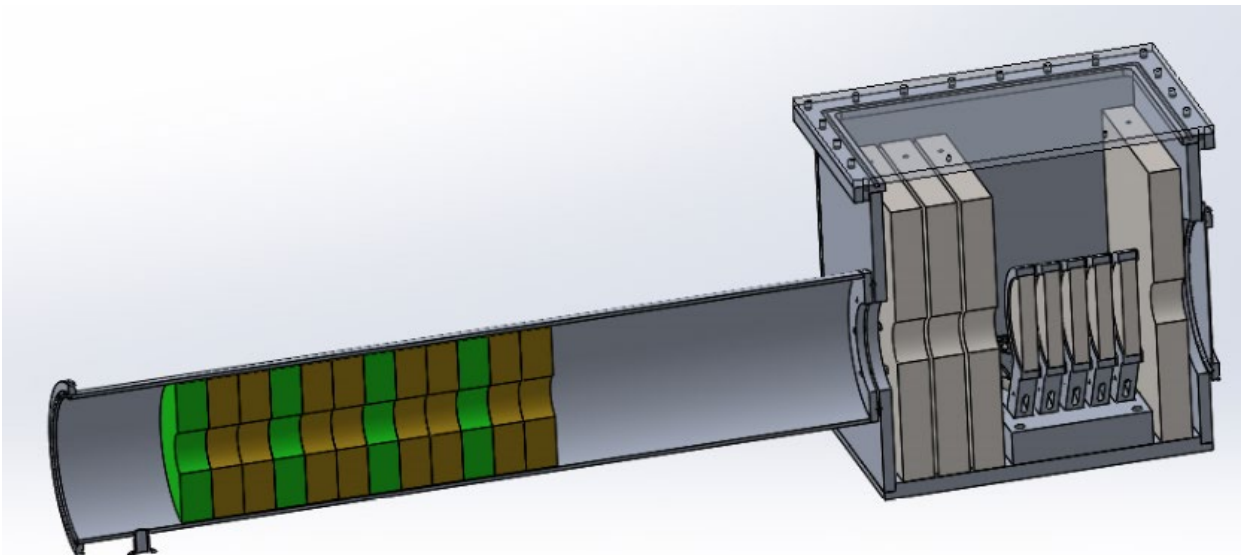


Figure 1. Cutaway drawing of the new DICER filter box and associated collimation. Five filters up to 1" thick can be remotely positioned in and out of the beam.

Third, the data acquisition and replay software is being upgraded to allow computer control of the new filter box (as well as other future devices such as a sample changer or beam blocker) and to make the system more logical.

V. Design studies for innovative dual-hole collimation system

Novel sample collimator designs which have the potential for minimizing the radioactive sample size are being explored. In previous neutron transmission experiments, the sample and an empty sample container (sample in and sample out) are cycled in and out of the beam; the flux-normalized ratio of these two measurements is the transmission T which is related to the total cross section σ_t by the equation $T = e^{-n\sigma_t}$, where n is the sample thickness. The neutron beam is collimated so that the detector (downstream of the sample) measures only those neutrons which traversed the sample. Because positioning systems have finite accuracy with which they can repeatedly locate the sample relative to the collimator, the sample size must be increased to ensure it subtends the entire beam defined by the collimator. If instead the sample does not move relative to the collimator, then the sample size can be minimized. This is important for radioactive samples because they can be extremely difficult to produce.

We currently are exploring two systems in which the sample remains fixed relative to the collimator. In both designs, the sample collimator has two holes; one for the sample and a second for the empty sample container. Both collimator holes are designed to point back to the same area on the neutron production target and hence transmit the same flux. In the first design, the collimator rotates so that

either the sample-in or sample-out collimator hole is aligned with the neutron source and detector (while the other hole is blocked). Thus, there are separate sample-in and sample-out measurements as in traditional transmission experiments. In the second design, the collimator is fixed and there are two operating options. In the first option, there is a movable beam blocker or shutter upstream of the sample collimator which is used to alternately block either the sample-in or sample-out collimator hole. Again there are both sample-in and sample-out measurements as in traditional transmission experiments. In the second option, both collimator holes are open and sample-in and sample-out measurements are performed simultaneously. In this case, either two detectors are needed or the detector must have enough imaging capability to differentiate between the flux transmitted through each collimator hole. In addition, there is potential for cross talk between the two detectors. However, this last option has the potential for halving the beam time need for a measurement.

We have done exploratory MCNP simulations of the last case described above and the results shown in Fig. 2 indicate that it should work. The two beam spots at the detector plane are sufficiently well separated so that the fluxes should be independently measureable. We hope to test this design during the current run cycle.

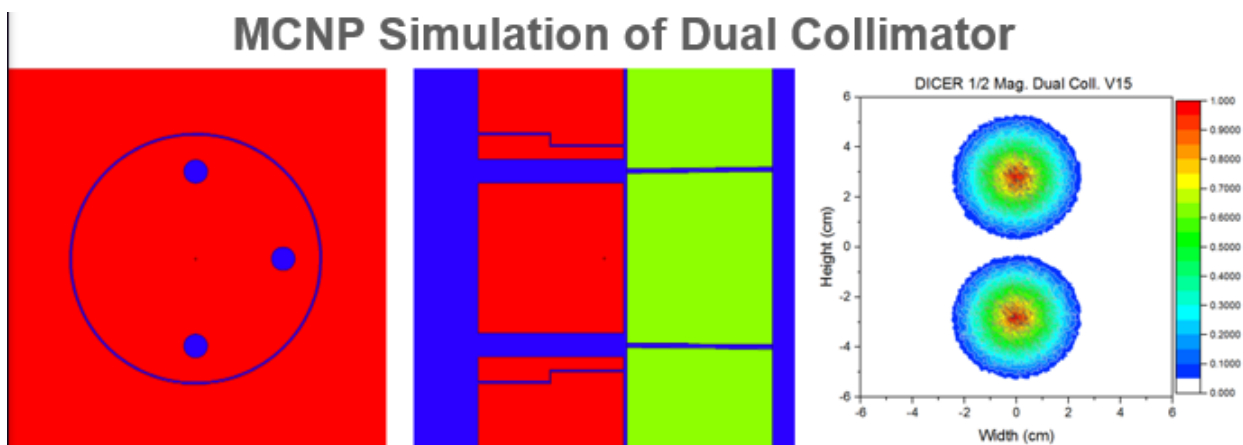


Figure 2. Candidate two-hole collimator design. The left drawing is a slice perpendicular to the neutron beam through the revolving beam blocker upstream of the collimator. It has three holes so that neither, one, or both of the collimator holes can be blocked. The middle drawing depicts a slice through this beam blocker (red) and collimator (green) along the beam direction, with the revolver rotated so that both collimator holes are open. The right panel is an MCNP mesh tally at the detector position 15 m downstream of the collimator. It indicates that the fluxes transmitted through the two collimator holes are well separated.

The sample collimator must be accurately aligned with the rest of the beam line. To this end, we are building a precision five-axis alignment system using parts from a decommissioned material-science instrument. A drawing of the main components of this system is shown in Fig. 3. This system also can be used to rotate the collimator between sample-in and sample-out positions as described in the first design above.

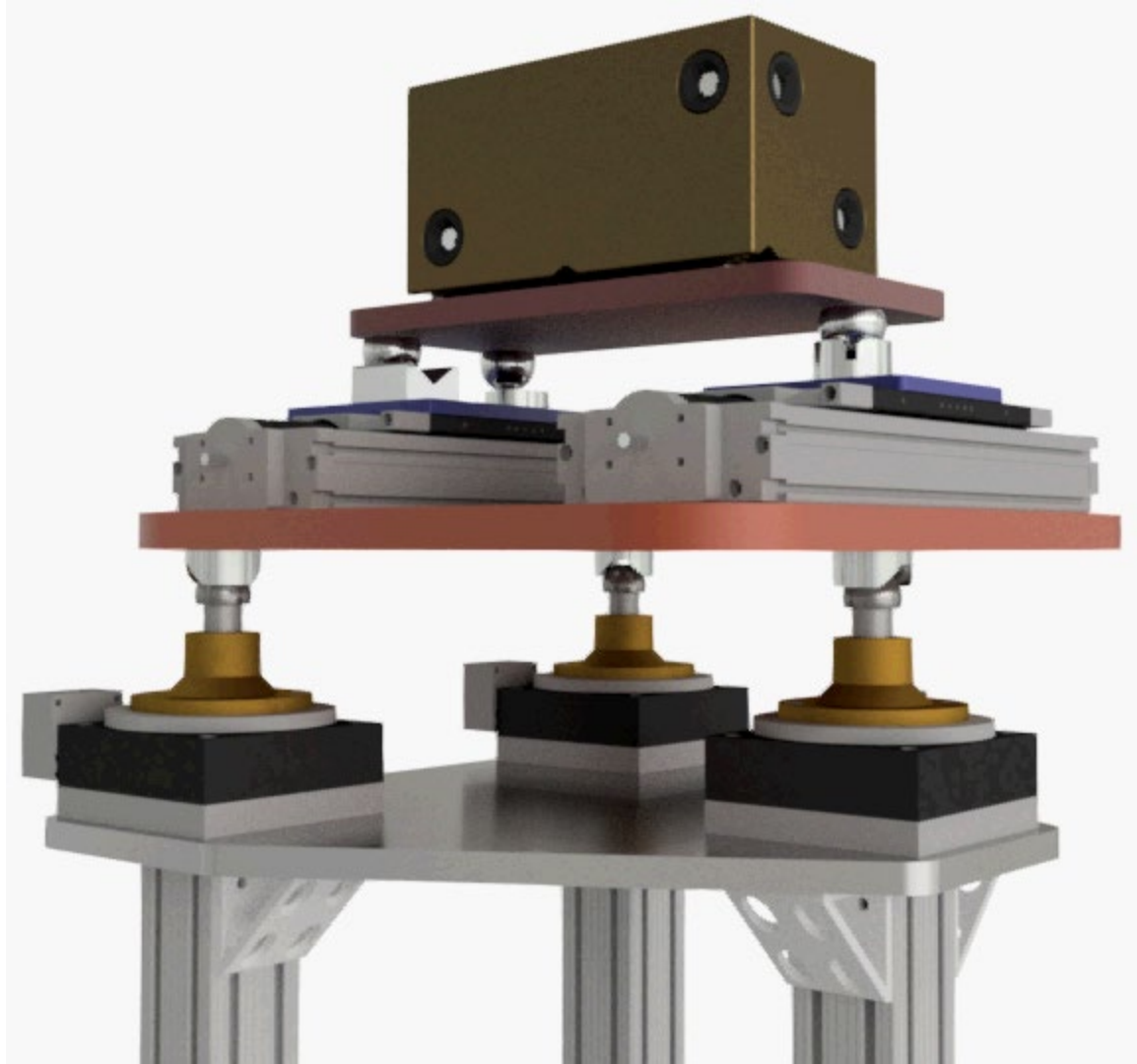


Figure 3. Three-dimensional rendering of the five-axis positioning system being built for the sample collimator. The collimator block and its alignment monuments sit atop the device.

VI. Uncertainty analysis and sensitivity study

As part of our LDRD DR proposal, we estimated the uncertainty in the $^{88}\text{Y}(n,\gamma)$ cross section before and after a DICER measurement. The before-DICER uncertainty was estimated using the five nuclear-level-density (NLD) and photon-strength-functions (PSF) models available in the nuclear statistical model (NSM) code Talys1.8 [2]. The resultant uncertainty in the $^{88}\text{Y}(n,\gamma)$ cross sections varies from a range of about a factor of five to 30 depending on the energy, and is shown by the red band in Fig. 4.

Calculating the uncertainty in the final $^{88}\text{Y}(n,\gamma)$ cross section due to uncertainties in the expected data and theory is straightforward and very similar to previous calculation we have done (e.g. [3]). The main difference in the present case is that we will be calibrating the NSM using measurements on the nuclide of interest rather than extrapolating or interpolating from data on nearby nuclides, and hence the current uncertainties will be smaller.

Of the three average resonance parameters obtained from a DICER experiment and subsequent R -matrix analysis, the resultant (n,γ) cross section is most sensitive to the average resonance spacing D . As a quantitative example, assume the $^{88}\text{Y}(n,\gamma)$ cross section is close to the current LANL value, which implies $D=21.5$ eV. Based on many years of experience and measurements with DICER so far, we can make high-quality transmission measurements to at least 1000 eV neutron energy using the planned 150 μg , 0.1 mm diameter sample. Hence, we expect to observe about $N=46$ ($1000/21.5$) resonances. The very conservative estimate that the well-known [4] relationship between N and the uncertainty in D is increased by 50% due to the well-known correction [5] for missed small resonances, leads to an expected 15% maximum uncertainty in D . To calculate the impact of this uncertainty on the (n,γ) cross section, the NLD model in Talys1.8 was adjusted to yield D values across this range and the resulting $^{88}\text{Y}(n,\gamma)$ cross sections calculated.

Other uncertainties were assessed in a similar fashion. Resulting uncertainties (which increase with energy) in the $^{88}\text{Y}(n,\gamma)$ cross section due to D , the average radiation width Γ_γ , the neutron strength function S , the NLD shape, and the PSF shape are 3.2 – 11.7, 1.6 – 6.0, ≈ 0 , 0.05 – 2.0, and 0.04 – 4.2%, respectively. Hence, the total expected uncertainty after a DICER measurement and analysis is about 4 – 14% (shown by the blue band in Fig. 4), much reduced from the current factor of 5 - 30. We discuss the impact of this greatly reduced uncertainty in the classified addendum to our LDRD DR proposal.

If the cross section is near the “Before DICER” lower limit shown in Fig. 4, the final uncertainty is larger. However, the smaller the cross section, the less destruction it causes and a larger uncertainty can be tolerated.

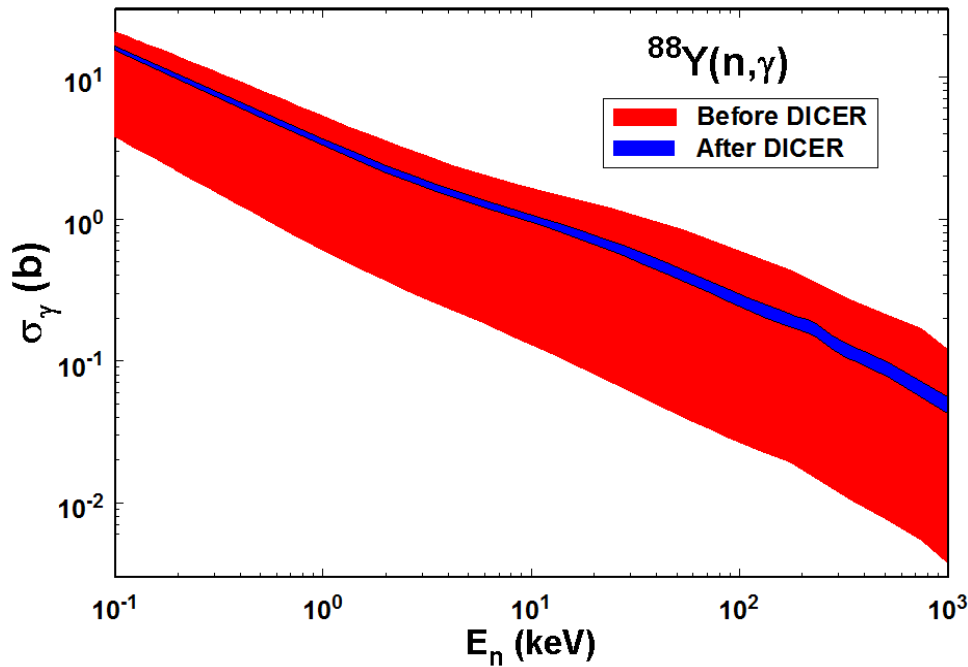


Figure 4. Estimated uncertainties in the $^{88}\text{Y}(n,\gamma)$ cross section before (red band) and after (blue band) a DICER measurement. See text for details.

VII. Assessment of the feasibility of a DICER ^{88}Zr measurement

It recently was reported [6] that the $^{88}\text{Zr}(n,\gamma)$ cross section at thermal energy (0.0253 eV) is an astounding 861 kb. This is the second largest thermal neutron capture cross section ever measured. Although this is an interesting curiosity, for applications the cross section is needed at higher energies. Presumably, this very large thermal cross section, which is orders of magnitude larger than the current LANL estimate, is due to a resonance very near thermal energy. As shown in Fig. 5, the location and width of this resonance has a large impact on the size and shape of the cross section at higher energies of importance to applications.

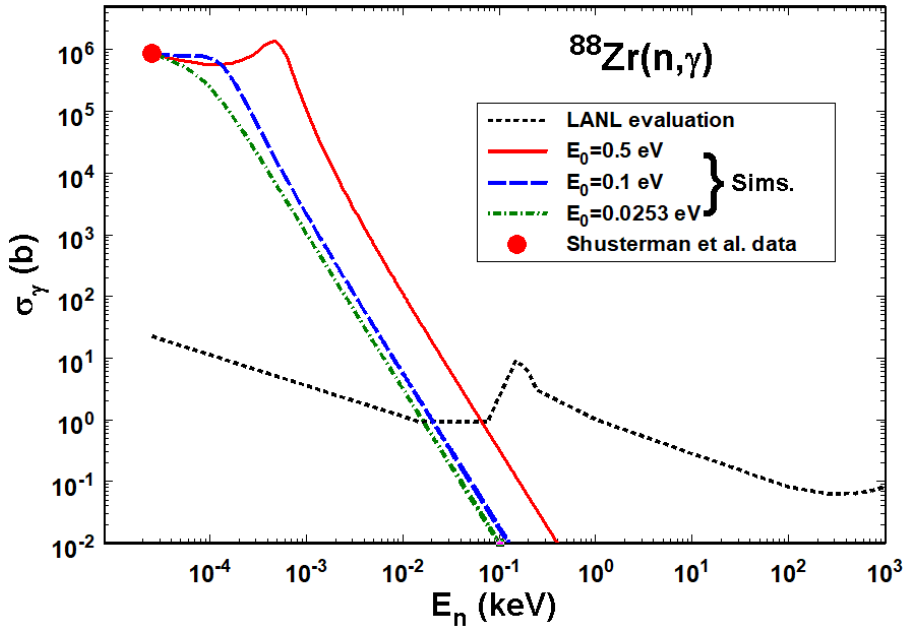


Figure 5. Measured (red circle) and LANL-evaluated (dashed black curve) $^{88}\text{Zr}(n,\gamma)$ cross sections. Also shown are calculated cross sections due to three possible resonance locations and widths (solid red, long-dashed blue, and dot-dashed green curves), all of which produce the measured thermal cross section but very different behavior at higher energies important to applications.

During the previous LANSCE run cycle, we fielded a test experiment with a cadmium sample scaled to have approximately the same transmission as a 1-mm diameter, 1.1 μg ^{88}Zr sample. Cd also has a large resonance near thermal energy, so it is a reasonable surrogate for a ^{88}Zr measurement. Despite the fact that the 1-mm diameter collimator was fairly crude and the sample-in to sample-out normalization was only approximate, the results shown in Fig. 6 are very encouraging; The resulting transmission, which took only a day to measure, is in agreement with the latest ENDF evaluation to very good precision. Also shown in this figure are expected transmission curves for a 1.1 μg , 1 mm diameter ^{88}Zr sample for the same three possible resonances shown in Fig. 5, which all result in the same reported thermal $^{88}\text{Zr}(n,\gamma)$ cross section of 861 kb, but very different cross sections at higher energies. We will be able to pinpoint the energy and width of the resonance responsible for the large thermal cross section and hence determine the shape of the cross section to higher energies important for applications.

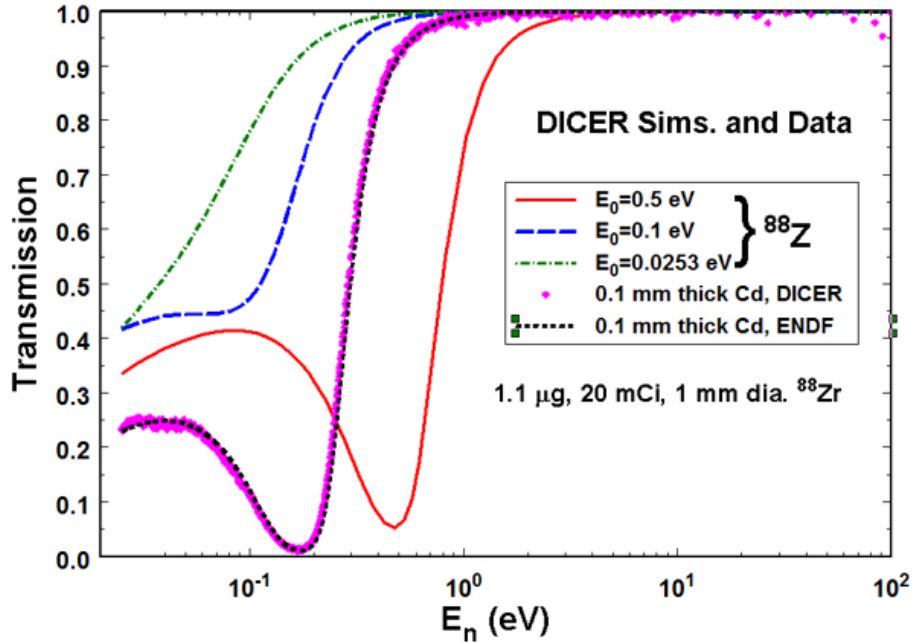


Figure 6. DICER-measured transmission versus energy for a 1-mm diameter Cd sample (magenta diamonds) whose thickness was scaled to have about the same transmission as expected for a 1.1 μg , 1-mm diameter ^{88}Zr sample. Transmission calculated with the latest ENDF parameters (short-dashed black curve) are in excellent agreement with these data. Also shown (solid red, long-dashed blue, and dot-dashed green curves) are expected transmissions for the mentioned ^{88}Zr sample assuming the same three resonances shown in Fig. 5. As can be seen, it is expected to be relatively easy to discern the energy and widths of this resonance using DICER.

VIII. DICER publications and talks

A paper entitled “Attempting to close the loop on the Oslo technique at ^{198}Au : Constraining the nuclear spin distribution” was accepted for publication in the proceedings of the 6th Workshop on Compound Nuclear Reactions. DICER data and analysis was instrumental to this work.

A talk entitled “Impact of Nuclear Data on NDSE and Radiochemical Diagnostics” was presented at the 10th Tri-Lab Nuclear Data Workshop in Livermore, CA on September 10, 2019. DICER simulations and analyses formed the bulk of this presentation.

References

- [1] LDRD DR 20200108.
- [2] A. J. Koning, S. Hilaire, and M. C. Duijvestijn, in *Proceedings of the International Conference on Nuclear Data for Science and Technology - ND2007*, edited by O. Bersillon *et al.* (EDP Sciences, Les Ulis, France, 2008), p. 211.
- [3] P. E. Koehler and K. H. Guber, *Phys. Rev. C* **88**, 035802 (2013).
- [4] S. F. Mughabghab, *Atlas of Neutron Resonances: Resonance Parameters and Thermal Cross Sections Z=1 – 100* (Elsevier, Amsterdam, 2006).
- [5] T. Fuketa and J. A. Harvey, *Nucl. Instrum. and Methods* **33**, 107 (1965).
- [6] J. A. Shusterman *et al.*, *Nature* **565**, 328 (2019).